International Journal of Bridge Engineering (IJBE), Vol. 8, No. 2, (2020), pp. 57-81

FLEXURE OF DEEP RECTANGULAR BEAMS WITH DIFFERENT BOUNDARY CONDITIONS

Yuwaraj M. Ghugal[1] and Ajay G. Dahake[2]

[1] Department of Applied Mechanics, Government College of Engineering, Karad-415124, Maharashtra, India
[2] Department of Civil Engineering, G H Raisoni College of Engineering and Management, Pune-412207, Maharashtra, India
e-mail: ymghugal@gmail.com, ajaydahake@gmail.com

ABSTRACT: The paper presents the exact analytical solutions for built-in and simply supported end conditions of uniform, isotropic deep beams using sinusoidal refined shear deformation theory (SSDT) under transverse bending. The theory is built upon the classical beam theory including sinusoidal function in terms of thickness coordinate to include the shear deformation effects. The kinematics of the theory enforces transverse shear stress to satisfy the shear stress-free conditions on the top and bottom planes of the beam. The shear stress distribution through the thickness is realistic and requires no shear correction factor. Using the principle of virtual work, the equilibrium equations and boundary conditions have been obtained based on kinematics of the theory. To demonstrate the efficacy of the theory, the exact analytical solutions for beams, with narrow rectangular cross sections, subjected to linearly varying load, parabolic load and cosine load are obtained to examine the complete flexural response. Results obtained are discussed critically with those of other theories. The solutions obtained can be served as a benchmark for comparison of results by other refined theories.

KEYWORDS: Deep beam, Sinusoidal shear deformation, Principle of virtual work, Equilibrium equations, Support conditions.

1 INTRODUCTION

Beam theories are widely used in structural analysis of slender bodies, such as columns, arches, blades, aircraft wings and fuselage, long ships, and bridges. The beam theory reduces the three-dimensional problem to a one-dimensional one based on the neutral axis coordinate of the beam. The theories based on such reductions are simpler and more efficient compared to two and three-dimensional theories. This virtue makes beam theories very attractive for the static and dynamic analysis of structures.

Bernoulli-Euler [1-4] developed the widely used classical or elementary theory

of beam bending almost 300 years ago. The historical development of this beam theory is given by Love [5]. The elementary theory of beam bending (ETB) is founded on the hypothesis that the plane sections remain plane and normal to the axis after bending, implying that the transverse shear and transverse normal strains are zero. Since theory neglects the transverse shear deformation, it is applicable for the analysis of slender beams. It underpredicts deflections in case of deep beams where shear deformation effects are significant.

Timoshenko [6] developed the first order shear deformation theory (FSDT) including rotatory inertia and shear deformation. In this theory transverse shear strain distribution is assumed to be constant across the beam thickness and requires shear correction factor to appropriately represent the strain energy of shear deformation. Further, FSDT does not satisfy the boundary condition of slope of deflection curve at the clamped support and needs to be revised to resolve this boundary condition paradox.

The discrepancies in classical and first order shear deformation theories led to the development of higher order or refined shear deformation theories for static and dynamic analysis of shear deformable beams. The methods of development of these theories are presented in Ghugal and Shimpi [7], Carrera et al. [8].

The higher order (third order) shear deformation theories of beams in terms of thickness coordinate, are developed by Levinson [9], Bickford [10], Rehfield and Murty [11], Krishna Murty [12], Baluch *et al*. [13], Bhimaraddi and Chandrashekhara [14] and Heyliger and Reddy [15]. These theories satisfy shear stress free boundary conditions on top and bottom surfaces of beam obviating the need of shear correction factor. However, the issues of bending and transverse shear stress distributions at the clamped boundary are not discussed.

The refined theories including trigonometric and hyperbolic functions to represent the shear deformation effects through the thickness also exist in the literature. Vlasov and Leont'ev [16] and Stein [17] developed refined shear deformation theories for thick beams including sinusoidal function in kinematics of the theory. However, shear stress free boundary conditions are not satisfied at top and bottom surfaces of the beam with these theories. Ghugal and Sharma [18, 19] developed a hyperbolic shear deformation theory for the static and dynamic analysis of thick beams. Ghugal and Dahake [20], Dahake and Ghugal [21] employed the refined shear deformation theory for flexure of thick simply supported and cantilever beams. Dufort et al. [22] obtained the closed-form solution for the cross-section warping in short beams under three-point bending using higher order theories.

Filon [23] obtained the realistic shear stress distribution due to concentrated and uniform loads which simulates that variation at the built-in end. Coker [24] verified and validated this shear stress distribution across the depth of the beam experimentally using photo-elasticity. Hildebrand and Reissner [25] studied

bending and shear stress distributions at the built-in end of the cantilever beams of narrow rectangular cross section using plane stress theory and the principle of least work. It is shown that the distribution of stress near built-in end deviates appreciably from the one given by the elementary beam theory. Pearson [26], Carus Wilson [27] studied the influence of surface loading on the flexure beam.

Canales and Mantari [28] presented an analytical solution for static flexure of thick isotropic rectangular beams with different boundary conditions. However, the bending and transverse shear stress distributions have not been obtained at the built-in end to show the correctness of the method used.

Critical reviews of refined theories are presented by Ghugal and Shimpi [7] and Sayyad and Ghugal [29]. It is seen that the Navier type solutions for simply supported boundary conditions are extensively used in the literature. However, the analytical solutions for static flexure of deep beams with built-in ends and specialized loading conditions using refined shear deformation theories are very limited. To circumvent the limitation of Navier type solution, an exact solution procedure to solve boundary value problem is developed to account for any type of loading and boundary conditions. This paper presents the analytical solutions for the static flexure of deep beams with simply supported and built-in boundary conditions. The numerical results obtained are compared with other refined theories to validate the theory.

2 MATHEMATICAL FORMULATION

The beam under consideration as shown in Fig.1 occupies in $0-x-y-z$ Cartesian coordinate system the region:

$$0 \le x \le L\ ; \quad -\frac{b}{2} \le y \le \frac{b}{2}\ ; \quad -\frac{h}{2} \le z \le \frac{h}{2}$$

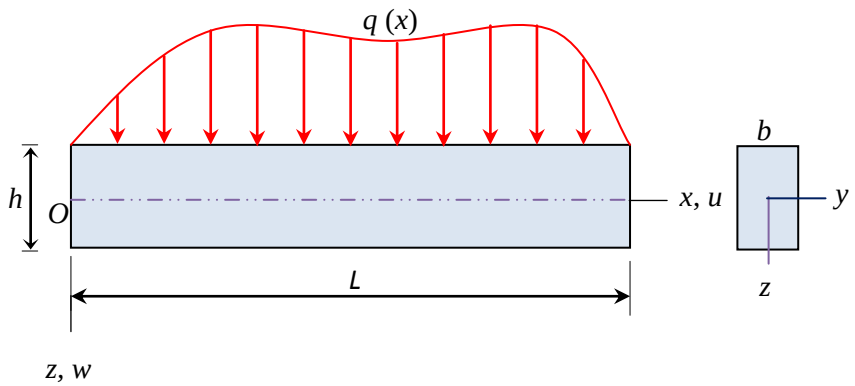

Figure 1. Beam under bending in *x*-*z* plane with cross section

where x, y, z are Cartesian coordinates, L and b are the length and width of

beam in the *x* and *y* directions respectively, and *h* is the thickness of the beam in the *z*-direction. The beam is made up of homogeneous, linearly elastic isotropic material.

2.1 The kinematics of the theory

The kinematics of the present beam theory is of the following form:

$$u(x,z) = -z\frac{dw}{dx} + \frac{h}{\pi}\sin\frac{\pi z}{h}\phi(x)$$
$$w(x,z) = w(x) \tag{1}$$

where u is the axial displacement in *x* direction and *w* is the transverse displacement in *z* direction. The sinusoidal function is assigned according to the shear stress distribution through the thickness of the beam. The ϕ represents rotation of the beam at neutral axis, which is an unknown function to be determined. The kinematics proposed in Eq. (1) is strongly based on solution of three-dimensional Navier's equations of elastostatics for thick plate under flexure presented by Green and Zerna [30] and Cheng [31] which involves transverse shear stress and transverse normal stress. The kinematics of proposed theory is the reduction problem from three-dimensional considerations to one-dimensional one. Hence, the theory represented by Eq. (1) is the correct deduction from the three- dimensional elasticity theory of thick plate. It is the simplest and richest refined beam theory with minimum number of unknown displacement variables. Theory based on this function enforces realistic cosinusoidal variation of transverse shear stress through the thickness of beam and obviates the need of shear correction factor.

The normal and shear strains are as follows:

Normal strain
$$\varepsilon_x = \frac{\partial u}{\partial x} = -z\frac{d^2w}{dx^2} + \frac{h}{\pi}\sin\frac{\pi z}{h}\frac{d\phi}{dx} \tag{2}$$

Shear strain
$$\gamma_{zx} = \frac{\partial u}{\partial z} + \frac{dw}{dx} = \cos\frac{\pi z}{h}\phi \tag{3}$$

The stress-strain relationships according to one dimensional Hooke's law are given by

$$\sigma_x = E\varepsilon_x \text{ and } \tau_{zx} = G\gamma_{zx} \tag{4}$$

where E and G are the elastic constants of the beam material.

2.2 Equilibrium equations and boundary conditions

Using the expressions for strains and stresses (2) through (4) and using the principle of virtual work, variationally consistent equilibrium equations and boundary conditions for the beam under consideration can be obtained. The

principle of virtual work when applied to the beam leads to:

$$b\int_{x=0}^{x=L}\int_{z=-h/2}^{z=+h/2}\left(\sigma_x\delta\varepsilon_x+\tau_{zx}\,\delta\gamma_{zx}\right)dx\,dz-\int_{x=0}^{x=L}q(x)\,\delta w\,dx=0 \tag{5}$$

where the symbol δ stands for a virtual variation. Employing Green's theorem in Eqn. (5) successively, we obtain the coupled Euler-Lagrange equations which are the equilibrium equations and associated boundary conditions of the beam. The equilibrium equations obtained are as follows:

$$EI\,\frac{d^4w}{dx^4}-\frac{24}{\pi^3}\,EI\,\frac{d^3\phi}{dx^3}=q(x) \tag{6}$$

$$\frac{24}{\pi^3}\,EI\,\frac{d^3w}{dx^3}-\frac{6}{\pi^2}EI\,\frac{d^2\phi}{dx^2}+\frac{GA}{2}\phi=0 \tag{7}$$

The boundary conditions (natural and forced) obtained at the ends $x = 0$ and $x = L$ are as follows:

$$\text{Either}\quad V_x=EI\,\frac{d^3w}{dx^3}-\frac{24}{\pi^3}\,EI\,\frac{d^2\phi}{dx^2}=0\quad\text{or } w\text{ is prescribed} \tag{8}$$

$$\text{Either}\quad M_x=EI\,\frac{d^2w}{dx^2}-\frac{24}{\pi^3}\,EI\,\frac{d\phi}{dx}=0\ \text{or}\ \frac{dw}{dx}\quad\text{is prescribed} \tag{9}$$

$$\text{Either}\quad M_s=EI\,\frac{24}{\pi^3}\,\frac{d^2w}{dx^2}-\frac{6}{\pi^2}\,EI\,\frac{d\phi}{dx}=0\quad\text{or }\phi\text{ is prescribed} \tag{10}$$

where V_x, M_x are the shear force and bending moment resultants respectively analogous to elementary theory of beam bending and M_s is the moment resultant because of transverse shear deformation. All the left-hand equations in Eqns. (8) to (10) are natural boundary conditions, and all the right-hand terms are the forced (rigid, kinematic, geometric) boundary conditions. The flexural behavior of the beam is described by the solution of these equations and simultaneously satisfaction of the associated boundary conditions. The boundary conditions for static flexure of beam under consideration can be obtained directly from Eqns. (8) through (10).

2.3 Analytical solution of equilibrium equations of the beam

The general solution for transverse displacement $w(x)$ and warping function $\phi(x)$ is obtained using Eqns. (6) and (7) using method of solution of linear differential equations with constant coefficients. Integrating and rearranging the first governing Eqn. (6), we obtain the following equation

$$\frac{d^3w}{dx^3}=\frac{24}{\pi^3}\frac{d^2\phi}{dx^2}+\frac{Q(x)}{EI} \tag{11}$$

where $Q(x)$ is the generalized shear force for beam and it is given by

$Q(x)=\int_0^x q dx + C_1$.

Now second governing Eqn. (7) is rearranged in the following form:

$$\frac{d^3w}{dx^3} = \frac{\pi}{4}\frac{d^2\phi}{dx^2} - \beta\phi \tag{12}$$

Using Eqns. (11) and (12), a single equation in terms of ϕ is now obtained as follows:

$$\frac{d^2\phi}{dx^2} - \lambda^2\phi = \frac{Q(x)}{\alpha EI} \tag{13}$$

where constants α, β and λ in Eqns. (12) and (13) are as follows

$$\alpha = \left(\frac{\pi}{4} - \frac{24}{\pi^3}\right),\ \beta = \left(\frac{\pi^3}{48}\frac{GA}{EI}\right) \text{and } \lambda^2 = \frac{\beta}{\alpha}$$

The general solution of Eqn. (13) is as follows:

$$\phi(x) = C_2\cosh\lambda x + C_3\sinh\lambda x - \frac{Q(x)}{\beta EI} \tag{14}$$

The equation of transverse displacement $w(x)$ is obtained by substituting the expression of $\phi(x)$ in Eqn. (14) and then integrating it thrice with respect to x. The general solution for $w(x)$ is obtained as follows:

$$EI\,w(x) = \iiint\int q\,dx\,dx\,dx\,dx + \frac{C_1x^3}{6} + \left(\frac{\pi}{4}\lambda^2 - \beta\right)\frac{EI}{\lambda^3}\left(C_2\sinh\lambda x + C_3\cosh\lambda x\right) + C_4\frac{x^2}{2} + C_5x + C_6 \tag{15}$$

where C_1, C_2, C_3, C_4, C_5 and C_6 are arbitrary constants and can be obtained by imposing natural (forced) and / or geometric or kinematical boundary / end conditions of beam.

3 ILLUSTRATIVE EXAMPLES

To prove the efficacy of the present theory, the four numerical examples are considered. The material properties for beam are as follows

E = 210 GPa, μ = 0.3 and ρ = 7800 Kg/m^3

where E is the Young's modulus, ρ is the density, and μ is the Poisson's ratio of beam material.

Example 1: A beam with built-in ends subjected to varying load,

A beam with built-in ends has its origin at left hand side support. The beam is subjected to varying load $q(x) = q_0\frac{x}{L}$ on surface z = +h/2 acting in the

downward *z* direction with maximum intensity of load q_0 as shown in Fig. 2.

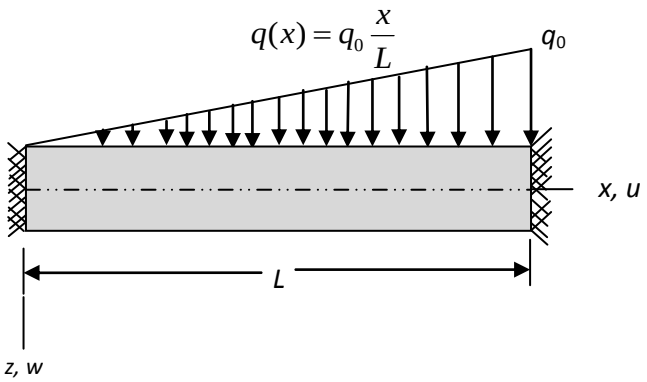

Figure 2. A beam with built-in ends subjected to varying load.

Following boundary conditions are used to obtained general solution:

At built-in ends: $\frac{dw}{dx} = \phi = w = 0$ at $x = 0, L$

General expressions using above boundary conditions obtained for $w(x)$ and $\phi(x)$ are as follows:

$$w(x) = \frac{q_0 L^4}{120EI}\left[\frac{x^5}{L^5} - 3\frac{x^3}{L^3} + 2\frac{x^2}{L^2} + \frac{9}{5}\frac{E}{G}\frac{h^2}{L^2}\left(\frac{5}{3}\frac{x^2}{L^2} - \frac{x}{L} + \frac{1+\sinh\lambda x - \cosh\lambda x}{\lambda L}\right)\right] \quad (16)$$

$$\phi(x) = \frac{q_0 L}{\beta EI}\left(1 - \frac{10}{3}\frac{x^2}{L^2} + \sinh\lambda x - \cosh\lambda x\right) \quad (17)$$

Substituting expressions for *w* and ϕ given by Eqns. (16) and (17) into Eqn. (1) through (4) the final expressions for axial displacement *u*, transverse displacement *w*, axial stresses σ_x and transverse shear stress τ_{zx} can be obtained respectively.

Expression for axial displacement, *u*

$$u = \frac{q_0 h}{Eb}\left\{\begin{array}{l} -\frac{z}{h}\frac{L^3}{h^3}\left[\frac{1}{2}\frac{x^4}{L^4} - \frac{9}{10}\frac{x^2}{L^2} + \frac{2}{5}\frac{x}{L} - \frac{9}{50}\frac{E}{G}\frac{h^2}{L^2}\left(\frac{10}{3}\frac{x}{L} - 1 + \cosh\lambda x - \sinh\lambda x\right)\right] \\ +\frac{36}{5\pi^4}\frac{E}{G}\frac{L}{h}\sin\frac{\pi z}{h}\left(-\frac{10}{3}\frac{x^2}{L^2} + 1 - \cosh\lambda x + \sinh\lambda x\right) \end{array}\right\} \quad (18)$$

Expression for axial stress, σ_x

$$\sigma_x = \frac{q_0}{b}\left\{\begin{array}{l} -\frac{z}{h}\left[\frac{L^2}{h^2}\left(2\frac{x^3}{L^3}-\frac{9}{5}\frac{x}{L}+\frac{2}{5}\right)-\frac{9}{50}\frac{E}{G}\left(\frac{10}{3}+\lambda L\,(\sinh\lambda x-\cosh\lambda x)\right)\right] \\ +\frac{36}{5\pi^4}\frac{E}{G}\sin\frac{\pi z}{h}\left(-\frac{20}{3}\frac{x}{L}+\lambda L(\cosh\lambda x-\sinh\lambda x)\right) \end{array}\right\} \quad (19)$$

Expression for transverse shear stress τ_{zx}^{CR} obtained from consecutive relationship:

$$\tau_{zx}^{CR} = \frac{36}{5\pi^3}\frac{q_0}{b}\frac{L}{h}\cos\frac{\pi z}{h}\left(1-\frac{10}{3}\frac{x^2}{L^2}+\sinh\lambda x-\cosh\lambda x\right) \quad (20)$$

Expression for transverse shear stress τ_{zx}^{EE} obtained from equilibrium equation:
It is obtained by integrating the stress equilibrium equation of two-dimensional elasticity theory and satisfying shear stress free boundary conditions on top and bottom surfaces of beam, which is as follows:

$$\frac{\partial\sigma_x}{\partial x}+\frac{\partial\tau_{zx}}{\partial z}=0 \quad (21)$$

$$\tau_{zx}^{EE} = \frac{q_0 L}{2bh}\left\{\begin{array}{l} \left(\frac{z^2}{h^2}-\frac{1}{4}\right)\left[6\frac{x^2}{L^2}-\frac{9}{5}-\frac{9}{50}\frac{E}{G}\frac{h^2}{L^2}\lambda^2L^2(\cosh\lambda x-\sinh\lambda x)\right] \\ +\frac{36}{5\pi^5}\frac{E}{G}\frac{h^2}{L^2}\cos\frac{\pi z}{h}\left(-\frac{20}{3}+\lambda^2L^2(\sinh\lambda x-\cosh\lambda x)\right) \end{array}\right\} \quad (22)$$

Example 2: A beam with built-in ends subjected to parabolic load,

A beam with built-in ends has its origin at left hand side support. The beam is subjected to parabolic load, $q(x)=q_0\left(1-\frac{x^2}{L^2}\right)$ on surface z = +*h*/2 acting in the downward *z* direction with maximum intensity of load q_0 as shown in Fig. 3.

General expressions obtained for $w(x)$ and $\phi(x)$ are as follows:

$$w(x) = \frac{q_0L^4}{120EI}\left[\begin{array}{l} 5\frac{x^4}{L^4}-\frac{1}{3}\frac{x^6}{L^6}+4\frac{x^2}{L^2}-\frac{26}{3}\frac{x^3}{L^3}-\frac{12}{\pi^2}\frac{E}{G}\frac{h^2}{L^2}\left(-\frac{1}{12}\frac{x^4}{L^4}+\frac{1}{6}\frac{x^2}{L^2}\right) \\ -\frac{26}{5}\frac{E}{G}\frac{h^2}{L^2}\left(-\frac{x}{L}+\frac{1}{2}\frac{x^2}{L^2}+\frac{\sinh\lambda x-\cosh\lambda x+1}{\lambda L}\right) \end{array}\right] \quad (23)$$

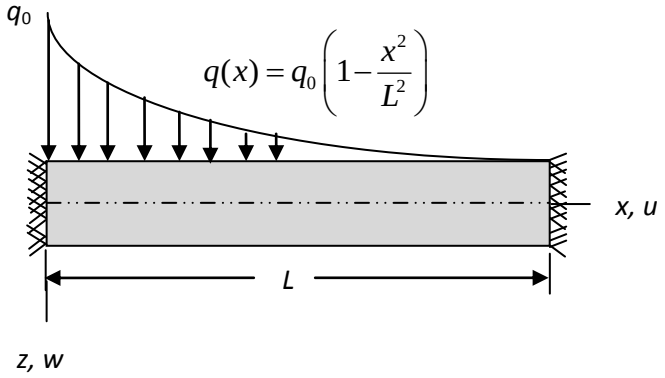

Figure 3. A beam with built-in ends subjected to parabolic load.

$$\phi(x) = \frac{q_0 L}{\beta EI}\frac{13}{30}\left(1+\frac{30}{13}\frac{x}{L}-\frac{10}{13}\frac{x^3}{L^3}+\sinh\lambda x-\cosh\lambda x\right) \tag{24}$$

The axial displacement and stresses obtained based on above solutions are as follows:

$$u = \frac{q_0 h}{Eb}\left\{\begin{array}{l} -\frac{1}{10}\frac{z}{h}\frac{L^3}{h^3}\left[\begin{array}{l} 20\frac{x^3}{L^3}-2\frac{x^5}{L^5}+8\frac{x}{L}-26\frac{x^2}{L^2}-\frac{12}{\pi^2}\frac{E}{G}\frac{h^2}{L^2}\left(-\frac{1}{3}\frac{x^3}{L^3}+\frac{1}{3}\frac{x}{L}\right) \\ -\frac{26}{5}\frac{E}{G}\frac{h^2}{L^2}\left(\frac{x}{L}-1+\cosh\lambda x-\sinh\lambda x\right) \end{array}\right] \\ -\frac{104}{5\pi^4}\sin\frac{\pi z}{h}\frac{E}{G}\frac{L}{h}\left(-\frac{10}{13}\frac{x^3}{L^3}+\frac{30}{13}\frac{x}{L}-1+\cosh\lambda x-\sinh\lambda x\right) \end{array}\right\} \tag{25}$$

$$\sigma_x = \frac{q_0}{b}\left\{\begin{array}{l} -\frac{1}{10}\frac{z}{h}\frac{L^2}{h^2}\left[\begin{array}{l} 60\frac{x^2}{L^2}-10\frac{x^4}{L^4}+8-52\frac{x}{L}-\frac{12}{\pi^2}\frac{E}{G}\frac{h^2}{L^2}\left(-\frac{x^2}{L^2}+\frac{1}{3}\right) \\ -\frac{26}{5}\frac{E}{G}\frac{h^2}{L^2}\left(1+\lambda L(\sinh\lambda x-\cosh\lambda x)\right) \end{array}\right] \\ -\frac{104}{5\pi^4}\sin\frac{\pi z}{h}\frac{E}{G}\left(\frac{30}{13}-\frac{30}{13}\frac{x^2}{L^2}+\lambda L(\sinh\lambda x-\cosh\lambda x)\right) \end{array}\right\} \tag{26}$$

$$\tau_{zx}^{CR} = \frac{104}{5\pi^3}\frac{q_0}{b}\frac{L}{h}\cos\frac{\pi z}{h}\left(1+\frac{10}{13}\frac{x^3}{L^3}-\frac{30}{13}\frac{x}{L}+\sinh\lambda x-\cosh\lambda x\right) \tag{27}$$

$$\tau_{zx}^{EE} = \frac{q_0 L}{80bh}\left(4\frac{z^2}{h^2}-1\right)\left[\begin{array}{l} 40\frac{x^3}{L^3}-120\frac{x}{L}-52+\frac{24}{\pi^2}\frac{E}{G}\frac{h^2}{L^2}\frac{x}{L} \\ -\frac{26}{5}\frac{E}{G}\frac{h^2}{L^2}\lambda^2L^2\left(\cosh\lambda x-\sinh\lambda x\right)\end{array}\right] \qquad (28)$$
$$-\frac{104}{5\pi^5}\cos\frac{\pi z}{h}\frac{E}{G}\frac{q_0 h}{bL}\left(\frac{60}{13}\frac{x}{L}+\lambda^2L^2\left(\cosh\lambda x-\sinh\lambda x\right)\right)$$

Example 3: Simply supported beam with cosine load,

The simply supported beam is having its origin at left support and is simply supported at x = 0 and x = L. The beam is subjected to cosine load, $q(x)=q_0\cos\frac{\pi x}{2L}$ on surface z = +h/2 acting in the downward z direction with maximum intensity of load q_0 as shown in Fig. 4.

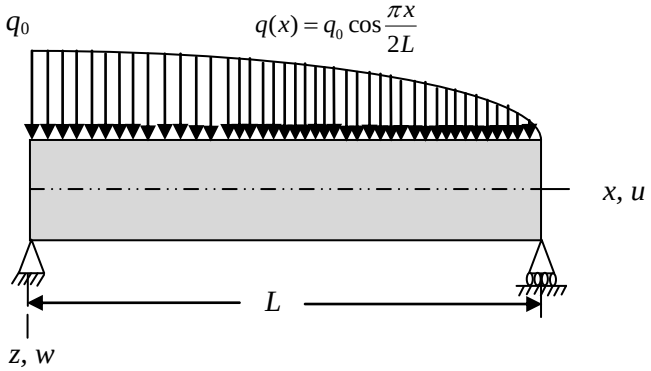

Figure 4. Simply supported beam with cosine load

Boundary conditions associated with this problem are as follows:

Simple Supports: $EI\frac{d^2w}{dx^2}=EI\frac{d\phi}{dx}=w=0$ at x = 0, L

General expressions obtained for transverse displacement $w(x)$ and shear rotation $\phi(x)$ are as follows:

$$w(x)=\frac{q_0L^4}{120EI}\left\{\begin{array}{l}\frac{480}{\pi^2}\left[\frac{4}{\pi^2}\left(\cos\frac{\pi x}{2L}-1+\frac{x}{L}\right)+\frac{1}{2}\frac{x^2}{L^2}-\frac{1}{6}\frac{x^3}{L^3}-\frac{1}{3}\frac{x}{L}\right]\\+\frac{11520}{\pi^6}\frac{E}{G}\frac{h^2}{L^2}\left(-\frac{1}{2}\frac{x^2}{L^2}+\frac{1}{2}\frac{x}{L}\right)\\+\frac{120}{\pi^2}\frac{E}{G}\frac{h^2}{L^2}\left(\frac{4}{\pi^2}\left(\cos\frac{\pi x}{2L}-1+\frac{x}{L}\right)+\frac{1}{2}\frac{x^2}{L^2}-\frac{1}{2}\frac{x}{L}\right)\end{array}\right\} \tag{29}$$

$$\phi(x)=\frac{q_0L}{\beta EI}\left(\frac{4}{\pi^2}-\frac{2}{\pi}\sin\frac{\pi x}{2L}+\frac{\sinh\lambda x-\cosh\lambda x}{\lambda L}\right) \tag{30}$$

The expressions for axial displacement and stresses obtained based on above solutions are as follows:

$$u=\frac{q_0h}{Eb}\left\{\begin{array}{l}-\frac{1}{10}\frac{z}{h}\frac{L^3}{h^3}\left(\begin{array}{l}\frac{480}{\pi^2}\left[\frac{4}{\pi^2}\left(-\frac{\pi}{2}\sin\frac{\pi x}{2L}+1\right)+\frac{x}{L}-\frac{1}{2}\frac{x^2}{L^2}-\frac{1}{3}\right]\\+\frac{11520}{\pi^6}\frac{E}{G}\frac{h^2}{L^2}\left(-\frac{x^2}{L^2}+\frac{1}{2}\right)\\+\frac{120}{\pi^2}\frac{E}{G}\frac{h^2}{L^2}\left(\frac{4}{\pi^2}\left(-\frac{\pi}{2}\sin\frac{\pi x}{2L}+1\right)+\frac{x}{L}-\frac{1}{2}\right)\end{array}\right)\\+\frac{48}{\pi^4}\sin\frac{\pi z}{h}\frac{E}{G}\frac{L}{h}\left(\frac{4}{\pi^2}-\frac{2}{\pi}\sin\frac{\pi x}{2L}+\frac{\sinh\lambda x-\cosh\lambda x}{\lambda L}\right)\end{array}\right\} \tag{31}$$

$$\sigma_x=\frac{q_0}{b}\left\{\begin{array}{l}-\frac{1}{10}\frac{z}{h}\frac{L^2}{h^2}\left[\frac{480}{\pi^2}\left[-\cos\frac{\pi x}{2L}+1-\frac{x}{L}\right]-\frac{11520}{\pi^6}\frac{E}{G}\frac{h^2}{L^2}+\frac{120}{\pi^2}\frac{E}{G}\frac{h^2}{L^2}\left(-\cos\frac{\pi x}{2L}+1\right)\right]\\+\frac{48}{\pi^4}\sin\frac{\pi z}{h}\frac{E}{G}\left(-\cos\frac{\pi x}{2L}+\cosh\lambda x-\sinh\lambda x\right)\end{array}\right\} \tag{32}$$

$$\tau_{zx}^{CR}=\frac{48}{\pi^3}\frac{q_0}{b}\frac{L}{h}\cos\frac{\pi z}{h}\left(\frac{4}{\pi^2}-\frac{2}{\pi}\sin\frac{\pi x}{2L}+\frac{\sinh\lambda x-\cosh\lambda x}{\lambda L}\right) \tag{33}$$

$$\begin{aligned}\tau_{zx}^{EE}=&\frac{q_0L}{80bh}\left(4\frac{z^2}{h^2}-1\right)\left[\frac{480}{\pi^2}\left(\frac{\pi}{2}\sin\frac{\pi x}{2L}-1\right)+\frac{120}{\pi^2}\frac{E}{G}\frac{h^2}{L^2}\left(\frac{\pi}{2}\sin\frac{\pi x}{2L}\right)\right]\\&+\frac{48}{\pi^5}\cos\frac{\pi z}{h}\frac{E}{G}\frac{q_0}{b}\frac{h}{L}\left(\frac{\pi}{2}\sin\frac{\pi x}{2L}+\lambda L(\sin\lambda x-\cosh\lambda x)\right)\end{aligned} \tag{34}$$

4 RESULTS AND DISCUSSION

4.1 Numerical results

In this paper, the results for axial displacement, transverse displacement, axial and transverse stresses are presented in the following non-dimensional form for the purpose of presenting the results in this work.

For beams subjected to various types of distributed loads, *q(x)*

$$\bar{u} = \frac{Ebu}{q_0 h}, \quad \bar{w} = \frac{10Ebh^3 w}{q_0 L^4}, \quad \bar{\sigma}_x = \frac{b\sigma_x}{q_0}, \quad \bar{\tau}_{zx} = \frac{b\tau_{zx}}{q_0}$$

The transverse shear stresses ($\bar{\tau}_{zx}$) are obtained by constitutive relation and by integration of equilibrium equation of two-dimensional elasticity and are denoted by ($\bar{\tau}_{zx}^{CR}$) and ($\bar{\tau}_{zx}^{EE}$) respectively. The transverse shear stress satisfies the stress-free boundary conditions on the top $\left(z = -h/2\right)$ and bottom $\left(z = +h/2\right)$ surfaces of the beam when both the above-mentioned approaches are used to obtain these stresses. Results obtained are presented in Tables 1 through 3 and in Figs. 5 through 16.

Table 1. Non-dimensional axial displacement ($\bar{u}$) at (x = 0.75L, z = h/2), transverse deflection ($\bar{w}$) at (x = 0.75L, z =0.0), axial stress ($\bar{\sigma}_x$) at (x = 0.0, z = h/2), maximum transverse shear stresses $\bar{\tau}_{zx}^{CR}$ at (x= 0.01L, z =0.0) and $\bar{\tau}_{zx}^{EE}$ at (x =0.01L, z =0.0) of the beam with built-in ends subjected to linearly varying load for aspect ratios (Example 1)

Source	*S*	Model	$\bar{u}$	$\bar{w}$	$\bar{\sigma}_x$	$\bar{\tau}_{zx}^{CR}$	$\bar{\tau}_{zx}^{EE}$
Present	4	SSDT	-2.2688	0.1761	5.1300	0.4426	-2.0074
Ghugal & Sharma [18, 19]		HPSDT	-1.6684	0.2591	6.5984	0.5229	-3.7170
Krishna Murty [12]		HSDT	-1.6670	0.2587	6.0172	0.4616	-2.2619
Timoshenko [6]		FSDT	-1.5375	0.2781	3.2000	0.0962	0.9000
Bernoulli-Euler [1-4]		ETB	-1.5375	0.1563	3.2000	—	0.9000
Present	10	SSDT	-25.8519	0.1598	25.9950	1.8617	-4.8045
Ghugal & Sharma [18, 19]		HPSDT	-22.4012	0.1730	28.4866	1.9906	-9.2855
Krishna Murty [12]		HSDT	-24.3472	0.1730	27.0928	1.8773	-5.6487
Timoshenko [6]		FSDT	-24.0234	0.1757	20.0000	1.5038	2.2500
Bernoulli-Euler [1-4]		ETB	-24.0334	0.1563	20.0000	—	2.2500

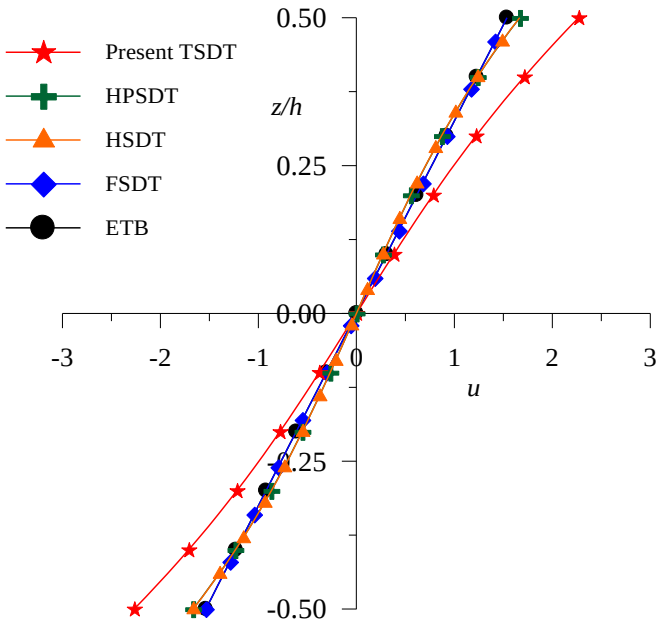

Figure 5. Variation of axial displacement ($\bar{u}$) through the thickness of beam with built-in ends at (x = 0.75L, z) when subjected to varying load for aspect ratio 4. (Example 1)

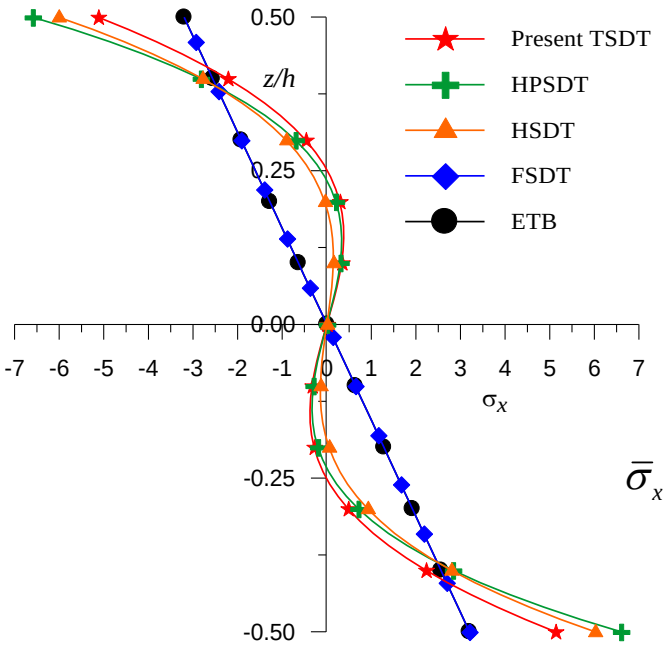

Figure 6. Variation of axial stress ($\bar{\sigma}_x$) through the thickness of beam with built-in ends at (x= 0, z) when subjected to varying load for aspect ratio 4. (Example 1)

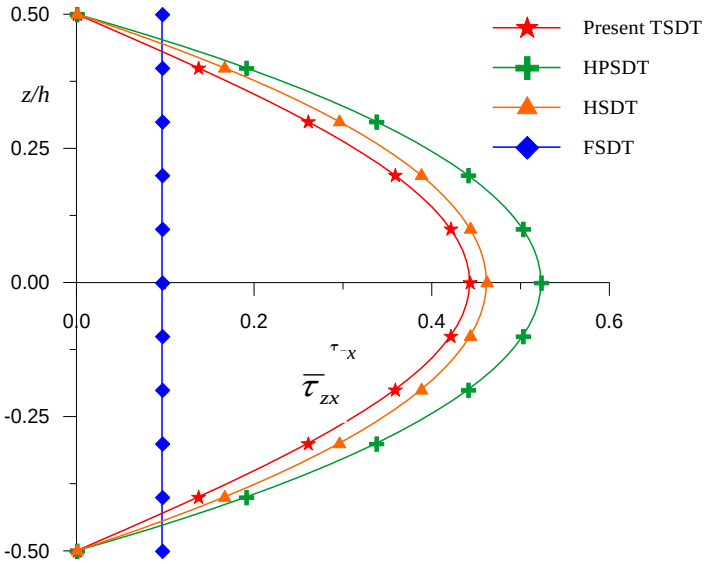

Figure 7. Variation of transverse shear stress ($\overline{\tau}_{zx}$) through the thickness of beam with built-in ends at (x = 0.01L, z) when subjected to varying load and obtain using constitutive relation for aspect ratio 4. (Example 1)

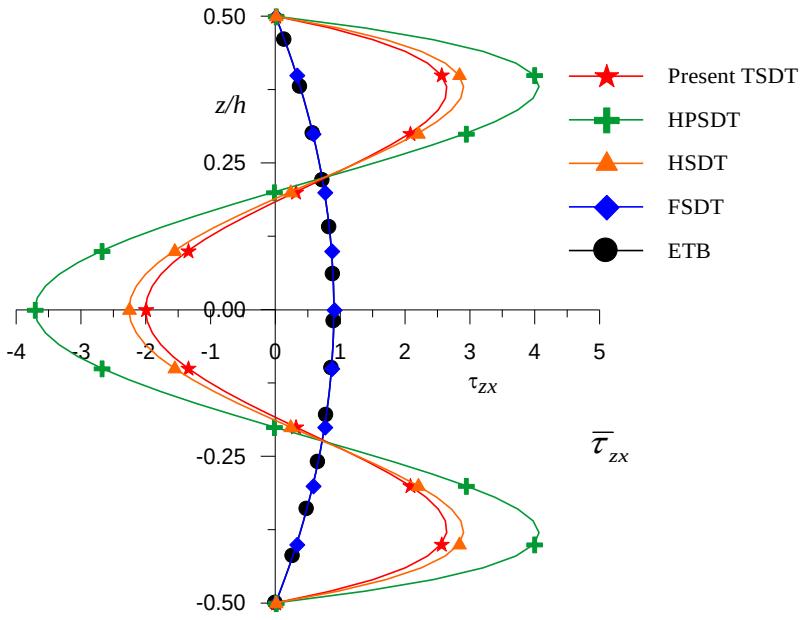

Figure 8. Variation of transverse shear stress ($\overline{\tau}_{zx}$) through the thickness of beam with built-in ends at (x = 0.01L, z) when subjected to varying load and obtain using equilibrium equation for aspect ratio 4. (Example 1)

Table 2. Non-dimensional axial displacement ($\bar{u}$) at (x=0.25l, z = h/2), transverse deflection ($\bar{w}$) at (x = 0.25L, z =0.0) axial stress ($\bar{\sigma}_x$) at (x =0, z = h/2) maximum transverse shear stresses $\bar{\tau}_{zx}^{CR}$ and $\bar{\tau}_{zx}^{EE}$ (x=0.01l, z =0.0) of the beam with built-in ends am subjected to parabolic load for aspect ratios (Example 2)

Source	S	Model	$\bar{u}$	$\bar{w}$	$\bar{\sigma}_x$	$\bar{\tau}_{zx}^{CR}$	$\bar{\tau}_{zx}^{EE}$
Present	4	SSDT	3.2032	0.3036	14.7191	5.6035	-1.8316
Ghugal and Sharma [18, 19]		HPSDT	2.6673	0.2893	16.3009	5.2756	-3.0137
Krishna Murty [12]		HSDT	2.7480	0.2965	14.6098	5.2259	-1.9020
Timoshenko [6]		FSDT	2.1937	0.1943	6.4000	2.9776	2.5400
Bernoulli-Euler [1-4]		ETB	2.1937	0.1340	6.4000	—	2.5400
Present	10	SSDT	3.2032	0.1624	59.9676	5.2259	2.2143
Ghugal and Sharma [18,19]		HPSDT	2.6673	0.1598	64.6002	5.6035	2.6138
Krishna Murty [12]		HSDT	2.7480	0.1611	60.3778	5.2756	2.5787
Timoshenko [6]		FSDT	2.1937	0.1437	40.0000	2.9777	6.3500
Bernoulli-Euler [1-4]		ETB	2.1937	0.1340	40.0000	—	6.3500

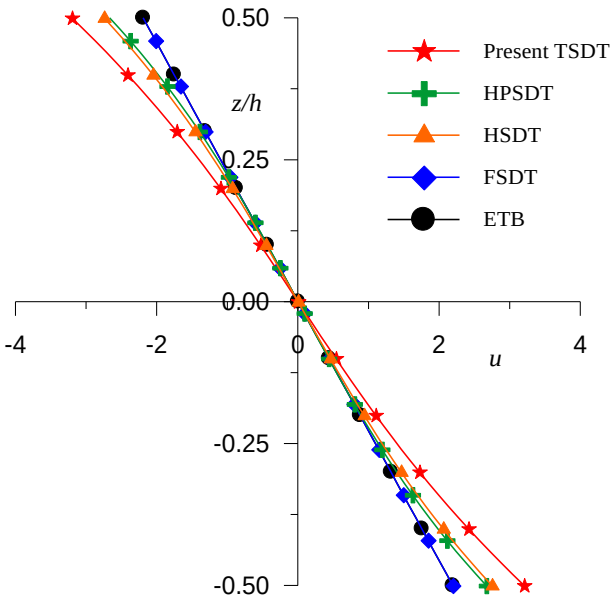

Figure 9. Variation of axial displacement ($\bar{u}$) through the thickness of beam with built-in ends at (x = 0.75L, z) when subjected to parabolic load for aspect ratio 4. (Example 2)

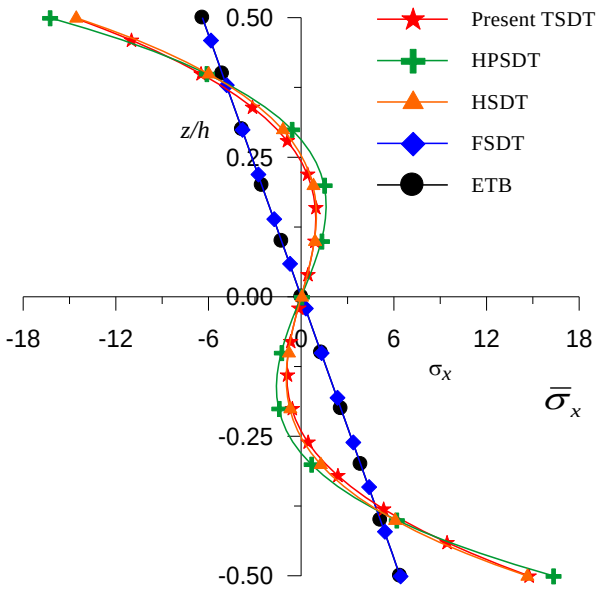

Figure 10. Variation of axial stress ($\overline{\sigma}_x$) through the thickness of beam with built-in ends at (x = 0, z) when subjected to parabolic load for aspect ratio 4. (Example 2)

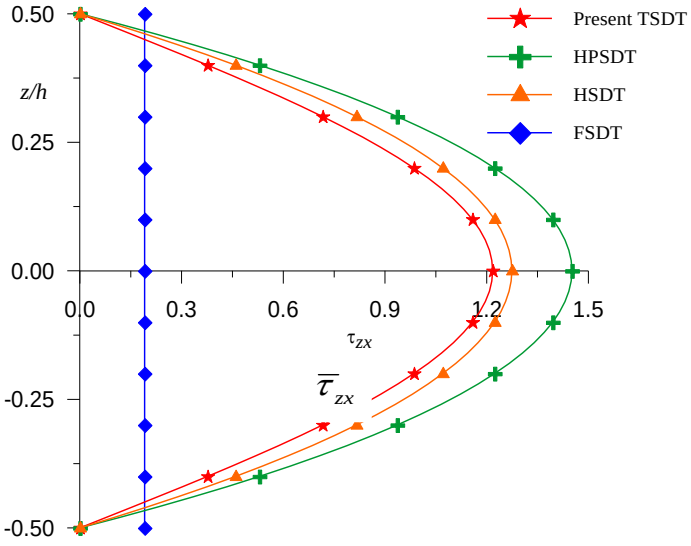

Figure 11. Variation of transverse shear stress ($\overline{\tau}_{zx}$) through the thickness of beam with built-in ends at (x = 0.01L, z) when subjected to parabolic load and obtain using constitutive relation for aspect ratio 4. (Example 2)

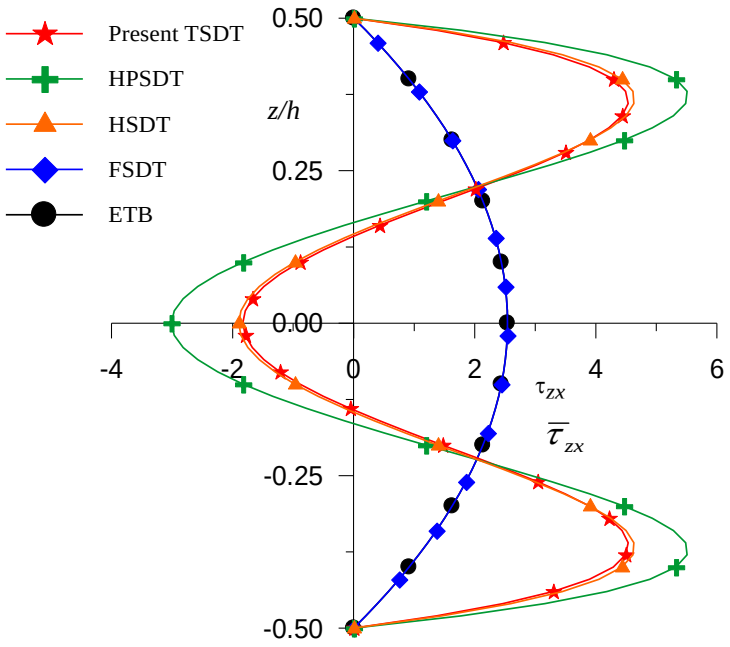

Figure 12. Variation of transverse shear stress ($\overline{\tau}_{zx}$) through the thickness of beam with built-in ends at (x = 0.01L, z) when subjected to parabolic load and obtain using equilibrium equation for aspect ratio 4. (Example 2)

Table 3. Non-dimensional axial displacement ($\overline{u}$) at (x=0.25l, z = h/2), transverse deflection ($\overline{w}$) at (x = 0.25l, z =0.0) axial stress ($\overline{\sigma}_x$) at (x =0, z = h/2) maximum transverse shear stresses $\overline{\tau}_{zx}^{CR}$ and $\overline{\tau}_{zx}^{EE}$ (x=0.01l, z =0.0) of the simply supported beam subjected to cosine load for aspect ratios (Example 3)

Source	S	Model	$\overline{u}$	$\overline{w}$	$\overline{\sigma}_x$	$\overline{\tau}_{zx}^{CR}$	$\overline{\tau}_{zx}^{EE}$
Present	4	SSDT	7.4974	0.9041	-7.0189	2.4140	-4.1749
Ghugal & Sharma [18, 19]		HPSDT	7.4893	0.9046	-7.0039	2.3557	-6.4511
Krishna Murty [12]		HSDT	7.4882	0.9046	-7.0039	2.3483	-4.8807
Timoshenko [6]		FSDT	7.3266	0.9050	-6.7651	2.1534	2.4317
Bernoulli-Euler [1-4]		ETB	7.3266	0.7676	-6.7651	—	2.4317
Present	10	SSDT	114.9057	0.7894	-42.5361	6.1785	-0.5273
Ghugal & Sharma [18, 19]		HPSDT	114.8855	0.7895	-42.5202	5.9918	-2.8035
Krishna Murty [12]		HSDT	114.8828	0.7895	-42.5212	5.9959	-1.2332
Timoshenko [6]		FSDT	114.8828	0.7895	-42.2824	1.3458	6.0792
Bernoulli-Euler [1-4]		ETB	114.4789	0.7676	-42.2824	—	6.0792

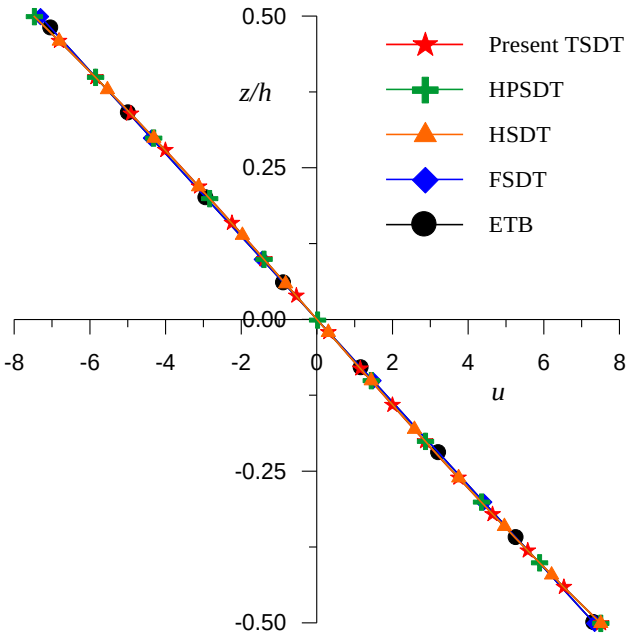

Figure 13. Variation of axial displacement ($\bar{u}$) through the thickness of simply supported beam at (x = 0.25L, z) when subjected to cosine load for aspect ratio 4. (Example 3)

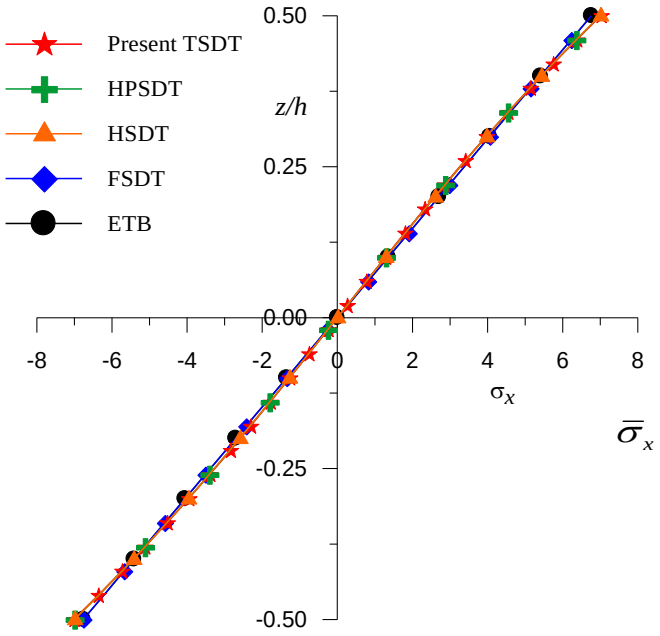

Figure 14. Variation of axial stress ($\bar{\sigma}_x$) through the thickness of simply supported beam at (x = 0.25L, z) when subjected to cosine load for aspect ratio 4. (Example 3)

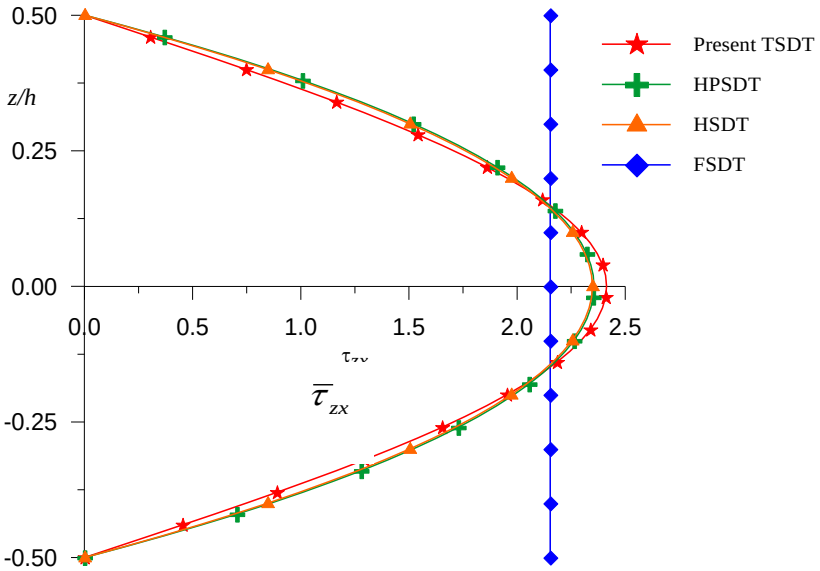

Figure 15. Variation of transverse shear stress ($\overline{\tau}_{zx}$) through the thickness of simply supported beam at (x = 0, z) when subjected to cosine load and obtain using constitutive relation for aspect ratio 4. (Example 3)

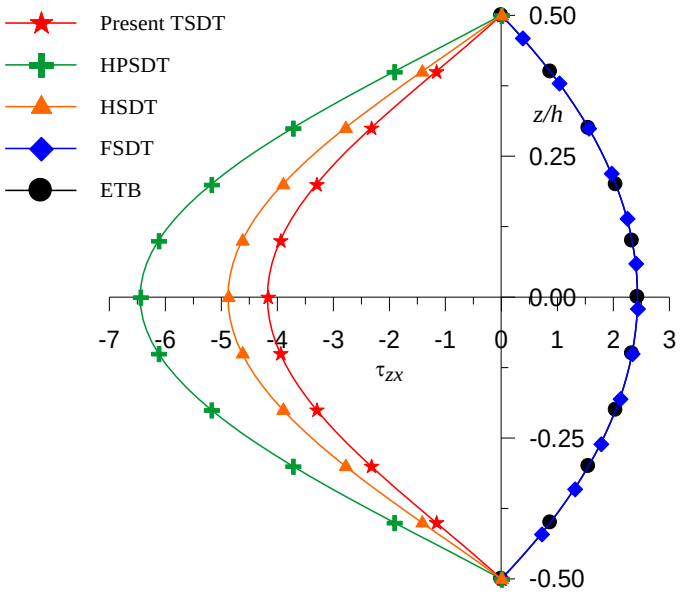

Figure 16. Variation of transverse shear stress ($\overline{\tau}_{zx}$) through the thickness of simply supported beam at (x = 0, z) when subjected to cosine load and obtain using equilibrium equation for aspect ratio 4. (Example 3)

4.2 Discussion of results

The results obtained from the present sinusoidal or trigonometric shear deformation theory (SSDT/TSDT) are compared with those of the elementary beam theory (ETB) [1-4], first order shear deformation theory (FSDT) of Timoshenko [6], higher order shear deformation theories (HSDT) of Krishna Murty [12] and hyperbolic shear deformation theory (HPSDT) of Ghugal and Sharma [18, 19]. The results in this section are discussed with respect to each example.

Example 1: The comparison of results of maximum non-dimensional axial displacement ($\bar{u}$) for the aspect ratios of 4 and 10 is presented in Table 1 for the beam with built-in ends subjected to linearly varying load (see Fig. 2). The values of axial displacement given by present theory are in close agreement with the values of other refined theories for aspect ratio 4 and 10. The through thickness distribution of this displacement obtained by present theory is in close agreement with other refined theories except the one given by classical and first order shear deformation theory (FSDT) as shown in Fig. 5 for aspect ratio 4.

The comparison of results of maximum non-dimensional transverse displacement ($\bar{w}$) for the aspect ratios of 4 and 10 is presented in Table 1. Among the results of all the other theories, the values of present theory are in good agreement with the values of other refined theories for aspect ratio 4 and 10 except those of classical beam theory (ETB) and FSDT of Timoshenko.

The results of axial stress ($\bar{\sigma}_x$) are shown in Table 1 for aspect ratios 4 and 10. The axial stresses given by present theory are compared with other higher order shear deformation theories. It is observed that the results by present theory are in good agreement with other refined theories. However, ETB and FSDT yield lower values of this stress as compared to the values given by other refined theories. The through the thickness variation of this stress given by ETB and FSDT is linear. Present and other higher order refined theories provide the non-linear variations of axial stress across the thickness at the built-in end due to heavy stress concentration. However, this effect of local stress concentration cannot be captured by lower order theories such as ETB and FSDT. The variations of this stress are shown in Fig. 6.

The comparison of maximum non-dimensional transverse shear stress for beams with built-in ends subjected to varying load obtained by the present theory and other refined theories is presented in Table 1 for aspect ratio of 4 and 10 respectively. The maximum transverse shear stress obtained by present theory using constitutive relation is in good agreement with that of higher order theory (HSDT), however HPSDT shows little departure from these theories for aspect ratio 4, and for aspect ratio 10 results of present theory and HSDT are in excellent agreement with each other. Among the values of this stress, the values obtained by HPSDT using equilibrium equation show considerable departure

from the values of present and HSDT. The values of present theory and those of HSDT are in good agreement with each other. The through thickness variations of this stress obtained via constitutive relation are presented graphically in Figs. 7 and those obtained via equilibrium equation are presented in Fig. 8. It can be seen from these figures that the nature of variation obtained by both the approaches is different from each other.

The through-the-thickness variation of this stress via equilibrium equation shows the anomalous behavior (changes its sign) due to heavy stress concentration associated with the built-in end of the beam which agrees with the photo-elasticity theory of Coker [24] and theory of Hildebrand and Reissner [25]. The maximum value of this stress does not occur at the neutral axis; however, it is observed to be shifted at $z = 0.375h$. The ETB and FSDT yield the identical values this stress at $z = 0$ and the variations across the thickness of the beam. It is seen that the anomalous behavior in the vicinity of built-in end cannot be captured by constitutive relation. Further, lower order theories, ETB and FSDT, cannot predict this behavior even with the use of equilibrium equation. Hence, the use of higher order or equivalent shear deformation theories is necessary to recover the effects of stress concentration at the built-in end of the beam with the use of equilibrium equation of two-dimensional theory of elasticity.

Example 2: The comparison of results of maximum non-dimensional axial displacement ($\bar{u}$) for the aspect ratios of 4 and 10 is presented in Table 2 for the beam with built-in ends subjected to parabolic load (see Fig. 3). The values of axial displacement given by present theory are in good agreement with the values of other refined theories for aspect ratio 4 and 10. The through-the-thickness distribution of this displacement obtained by present theory is in close agreement with other refined theories except the one given by classical and first order shear deformation theory (FSDT) as shown in Fig. 9 for aspect ratio 4.

The comparison of results of maximum non-dimensional transverse displacement ($\bar{w}$) for the aspect ratios of 4 and 10 is presented in Table 2. The values of present theory are in excellent agreement with the values of other refined theories for aspect ratio 4 and 10 except those of classical beam theory (ETB) and FSDT of Timoshenko.

The results of axial stress ($\bar{\sigma}_x$) are shown in Table 2 for aspect ratios 4 and 10. The axial stresses given by present theory are compared with other higher order shear deformation theories. It is observed that the results by present theory are in excellent agreement with those of HSDT of Krishna Murty [12]. However, ETB and FSDT yield lower values of this stress as compared to the values given by other refined theories. The through the thickness variation of this stress given by ETB and FSDT is linear. Present and other higher order refined theories provide the non-linear variations of axial stress across the

thickness at the built-in end due to heavy stress concentration. However, this effect of local stress concentration cannot be captured by lower order theories such as ETB and FSDT. The variation of this stress is shown in Fig. 10.

The comparison of maximum non-dimensional transverse shear stress is presented in Table 2 for aspect ratio of 4 and 10. The maximum transverse shear stresses obtained by present theory using constitutive relation are in good agreement with those of higher order theories. Among the values of this stress, the values obtained by HPSDT using equilibrium equation show considerable departure from the values of present and HSDT. The values of present theory and those of HSDT are in good agreement with each other. The through thickness variation of this stress obtained via constitutive relation is presented graphically in Fig. 11 and that is obtained via equilibrium equation is presented in Fig. 12. It can be seen from these figures that the nature of variation obtained by both the approaches is different from each other.

The through thickness variation of this stress via equilibrium equation shows the anomalous behavior (changes its sign) due to heavy stress concentration associated with the built-in end of the beam. The maximum value of this stress does not occur at the neutral axis; however, it is observed to be shifted at $z = 0.375h$. The ETB and FSDT yield the identical values of this stress at $z = 0$ and the variations across the thickness of the beam. It is seen that the anomalous behavior in the vicinity of built-in end cannot be captured by constitutive relation. Further, lower order theories, ETB and FSDT, cannot predict this behavior even with the use of equilibrium equation. Hence, the use of higher order or equivalent shear deformation theories is necessary to recover the effects of stress concentration at the built-in end of the beam with the use of equilibrium equation of two-dimensional theory of elasticity.

Example 3: The comparison of results of maximum non-dimensional axial and transverse displacements ($\bar{u}$) and ($\bar{w}$) for the aspect ratios of 4 and 10 is presented in Table 3 for the simply supported beam subjected to cosine load (see Fig. 4). The values of these displacements given by present theory are in excellent agreement with those of other refined theories for aspect ratio 4 and 10. The through-the-thickness distribution of axial displacement obtained by present theory is in close agreement with other refined theories as shown in Fig. 13 for aspect ratio 4.

The results of axial stress ($\bar{\sigma}_x$) are shown in Table 3 for aspect ratios 4 and 10. It is observed that the results obtained by present theory are in excellent agreement with those of other refined theories. However, ETB and FSDT show the little departure from the values of refined theories. The through the thickness variation of this stress given by refined and ETB and FSDT is linear. The variation of this stress is shown in Fig. 14.

The comparison of maximum non-dimensional transverse shear stress is

presented in Table 3 for aspect ratio of 4 and 10. The maximum transverse shear stresses obtained by present theory using constitutive relation are in excellent agreement with those of higher order theories. The through thickness variation of this stress obtained via constitutive relation is presented graphically in Fig. 15. The through thickness variation of this stress via equilibrium equation is shown in Fig. 16. The nature of this stress obtained by refined theories shows reversal of sign as compared to one obtained by ETB and FSDT. It can be seen from these figures that the nature of variation obtained by both the approaches is different from each other.

5 CONCLUSIONS

A sinusoidal refined shear deformation theory for flexure of rectangular deep beams with different support and loading conditions is presented. The results obtained are discussed with those of other refined theories. From the results and discussion of present study following conclusions are drawn.

1. The axial and the transverse displacements predicted by the present theory are in excellent in agreement with the other shear deformation theories. The distribution of axial displacement across the depth is non-linear and realistic.
2. The axial stresses and their distributions across the thickness of beam given by present theory are in excellent agreement with those of higher order shear deformation theories. The variation of this stress is non-linear through-the-thickness of beam.
3. The transverse shear stresses and their distributions through the thickness of beam obtained from constitutive relation are in close agreement with that of other higher order refined theories. Study, however, reveals that the use of constitutive relation cannot predict the effect of stress concentration in the neighbourhood of the built-in end of the beam.
4. The effect of stress concentration on variation of transverse shear stress is exactly predicted by the present theory with the use of equilibrium equation of two-dimensional elasticity. The realistic variations of these stresses at the built-in end of beams are presented. Hence, the use of equilibrium equation is inevitable to predict the effect stress concentration in accordance with the higher/ equivalent refined shear deformation theories.
5. The nature of shear stress distribution for a simply supported beam subjected to cosine load depicted the reversal of sign as compared to the one obtained by constitutive relation and the distributions obtained by ETB and FSDT using equilibrium equation.

In general, the use of present theory gives accurate results as seen from the numerical examples studied and it can predict the local effects in the vicinity of the built-in end of the deep beams. This validates the efficacy and credibility of refined sinusoidal shear deformation theory.

REFERENCES

[1] Bernoulli, J, "Curvatura laminae elasticae", Acta Eruditorum Lipsiae, Vol. 3, No. 6, pp. 262–276, 1694. Also reprinted in Jacobi Bernoulli, Basileensis, Opera. Tomus Primus (Vol. 1), No. LVIII (58), pp. 576-600, 1744.

[2] Bernoulli, J, "Explicationes, annotations et additions", Acta Eruditorum Lipsiae, pp. 537-553, 1695. Also reprinted in Jacobi Bernoulli Basileensis, Opera. (2 vols.), 1(LXVI), p. 639., 1744.

[3] Bernoulli, J, "Veritable hypothese de la resistance des solides, avec la demonstration de la corbure des corps qui font resort", *Histoire de l'Academie Royale des Sciences*, pp.176-186, 1705, Paris. Also reprinted in Jacobi Bernoulli, Basileensis, Opera. Tomus Secondus (Vol. 2), No. CII (102), pp. 976-989, 1744.

[4] Euler, L, *Methodus inveniendi lineas curvas maximi minimive proprietate gaudentes, sive solutio problematis isoperimetrici latissimo sensu accepti*, Apud Marcum-Michaelem Bousquet & Socio, Lausanne and Genevae, Switzerland, pp.1-322, 1744.

[5] Love, AEH, *The mathematical theory of elasticity*, Dover Publications, New York ,1944.

[6] Timoshenko, SP, "On the correction for shear of the differential equation for transverse vibrations of prismatic bars", Philosophical Magazine, Series 6, Vol. 41, Issue 245, pp. 744-746, 1921.

[7] Ghugal, YM, Shmipi, RP, "A review of refined shear deformation theories for isotropic and anisotropic laminated beams", Journal of Reinforced Plastics and Composites, Vol. 20, No. 3, pp. 255-272, 2001.

[8] Carrera, E, Giunta, G, Petrolo, M, *Beam Structures*: *Classical and Advanced Theories*, First Edition, Wiley, UK, 2011.

[9] Levinson, M, "A new rectangular beam theory", Journal of Sound and Vibration, Vol.74, No. 1, pp. 81-87, 1981.

[10] Bickford, WB, "A consistent higher order beam theory", *Procs. Developments in Theoretical and Applied Mechanics*, SETAM, Vol. 11: pp. 137-150, 1982.

[11] Rehfield, LW, Murthy, PLN, "Toward a new engineering theory of bending: fundamentals", AIAA Journal, Vol. 20, No. 5, pp. 693-699, 1982.

[12] Krishna Murty, AV, Towards a consistent beam theory. AIAA Journal 1984; 22(6): 811-816.

[13] Baluch, MH, Azad, AK, Khidir, MA, "Technical theory of beams with normal strain", ASCE Journal of Engineering Mechanics, Vol. 110, No. 8, pp. 1233-1237, 1984.

[14] Bhimaraddi, A, Chandrashekhara, K, "Observations on higher order beam theory", ASCE Journal of Aerospace Engineering, Vol. 6, No. 4, pp. 408-413, 1993.

[15] Heyliger, PR, Reddy, JN, "A higher order beam finite element for bending and vibration problems", Journal of Sound and Vibration, Vol. 126, No. 2, pp. 309-326, 1988.

[16] Vlasov, VZ, Leont'ev, UN, *Beams, plates and shells on elastic foundations*, Moskva, Chapter 1, pp. 1-8. Translated form the Russian by Barouch, A. and Plez, T., Israel Program for Scientific Translation Ltd., Jerusalem, 1966.

[17] Stein, M, "Vibration of beams and plate strips with three-dimensional flexibility", ASME Journal of Applied Mechanics Vol. 56, No. 1, pp. 228-231, 1989.

[18] Ghugal, YM, Sharma, R, "A hyperbolic shear deformation theory for flexure and vibration of thick isotropic beams", International Journal of Computational Methods, Vol. 6, No. 4, pp. 585-604, 2009.

[19] Ghugal, YM, Sharma, R, "A refined shear deformation theory for flexure of thick beams", Latin American Journal of Solids and Structures, Vol. 8, No. 2, pp.183-193, 2011.

[20] Ghugal, YM, Dahake, AG, "Flexural analysis of deep beams subjected to parabolic load using refined shear deformation theory", Applied and Computational Mechanics, Vol. 2, No. 2, pp. 163-172, 2012.

[21] Dahake, AG, Ghugal, YM, "A trigonometric shear deformation theory for flexure of thick beam", Procedia Engineering, Elsevier, Vol. 51, pp. 1-7, 2013.

[22] Dufort, L, Drapier, S, Grediac, M, "Closed-form solution for the cross-section warping in short beams under three-point bending", Composite Structures, Vol. 52, pp. 233-246, 2001.
[23] Filon, LNG, "On an approximate solution for the bending of a beam of rectangular cross-section under any system of load, with special reference to points of concentrated or discontinuous loading", Philosophical Transactions of the Royal Society of London, Series A, Vol. 201, pp. 63–155, 1903.
[24] Coker, EG, "An optical determination of the variation of stress in a thin rectangular plate subjected to shear", Proceedings of The Royal Society of London, Series A, Vol. 86, No. 587, pp. 291-319, 1912.
[25] Hildebrand, FB, Reissner, E, "Distribution of stress in built-in beam of narrow rectangular cross section", ASME Journal of Applied Mechanics, Vol. 64, pp.109-116, 1942.
[26] Pearson, Karl, "On the flexure of heavy beams subjected to continuous system of load", The Quarterly Journal of Pure and Applied Mathematics, Vol. 24, No. 93, pp. 63-96, 1889.
[27] Carus Wilson, CA, "The influence of surface loading on the flexure of beams", Philosophical Magazine, Series 5, Vol. 32, No.199, pp. 481-50, 1891.
[28] Canales, FG, Mantari, JL, "Boundary discontinuous Fourier analysis of thick beams with clamped and simply supported edges via CUF", Chinese Journal of Aeronautics, Vol. 30, No. 5, pp. 1708-1718, 2017.
[29] Sayyad, AS, Ghugal, YM, "Bending, buckling and free vibration of laminated composite and sandwich beams: A critical review of literature", Composite Structures, Vol. 171, pp. 486-504, 2017.
[30] Green, AE, Zerna, W, *Theoretical elasticity*, Second Edition, Oxford University Press, Ely House, London, 1968.
[31] Cheng, S., "Elasticity theory of plates and refined theory", ASME Journal of Applied Mechanics, Vol. 46, pp. 644-650, 1979.